Subsurface Investigation of Cape Kolka, Latvia: A Strandplain Along the Baltic Coast

Hailee Jefferies, Harry Jol, Donatas Pupienis, Martin Goettl, Cameron Wingren, Kelly Jerviss, Logan Bergevin, and Joseph Beck | Department of Geography and Anthropology

Introduction

The Cape Kolka is a strandplain, which contains a belt of sand ridges that are parallel and semi-parallel to the beach at 70 km in length and 10 km at its widest. This large strandplain has formed by large amounts of sediment being eroded along the sw coast by waves and longshore drift. It forms the western coastline of Latvia, Eastern Europe, where two seas meet- the Baltic Sea and the Gulf of Riga (figure 1). In the 20th century, the strandplain was zoned off as a Soviet military base that housed thousands of men and women who built small villages within, many of which are now abandoned. The study site was along a road used by Soviet officers to travel down towards the coast at the end of the road, where several buildings were built for officers and their families to enjoy the beach. These buildings can still be found today within the wooded areas close to the coast (figure 2). Cape Kolka is now part of the Slitere National Park, a protected nature reserve that is a popular tourist destination for sightseeing, hiking, and vacationing.

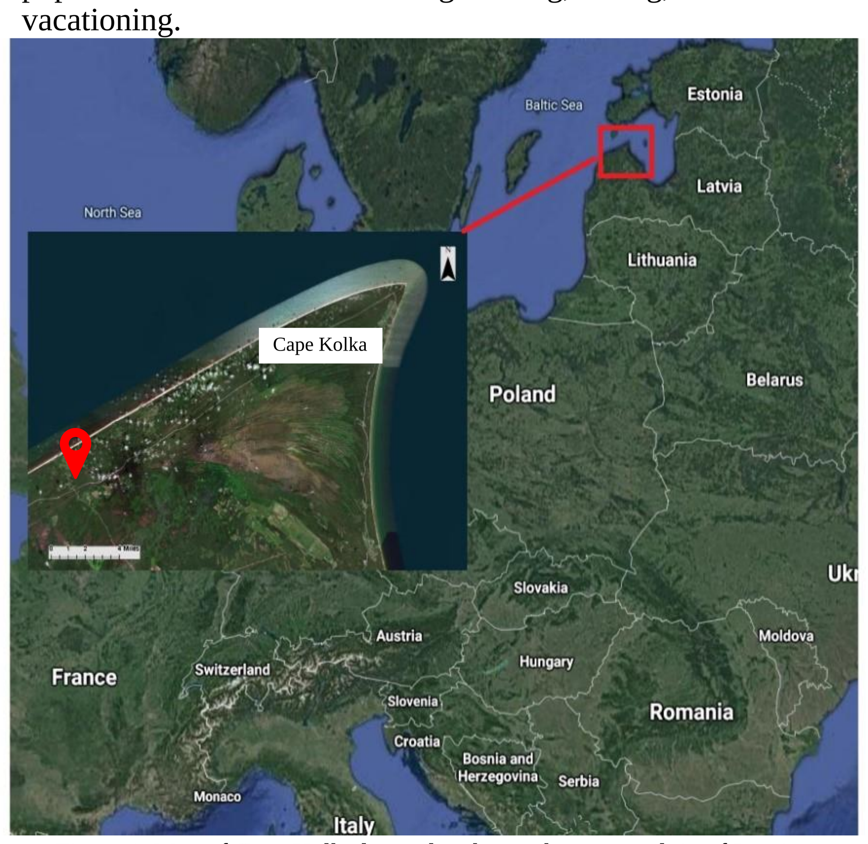

Figure 1. Map of Cape Kolka located at the northern coastal tip of Latvia, Eastern Europe, study site indicated with red pin. (Google Maps, 2020.)

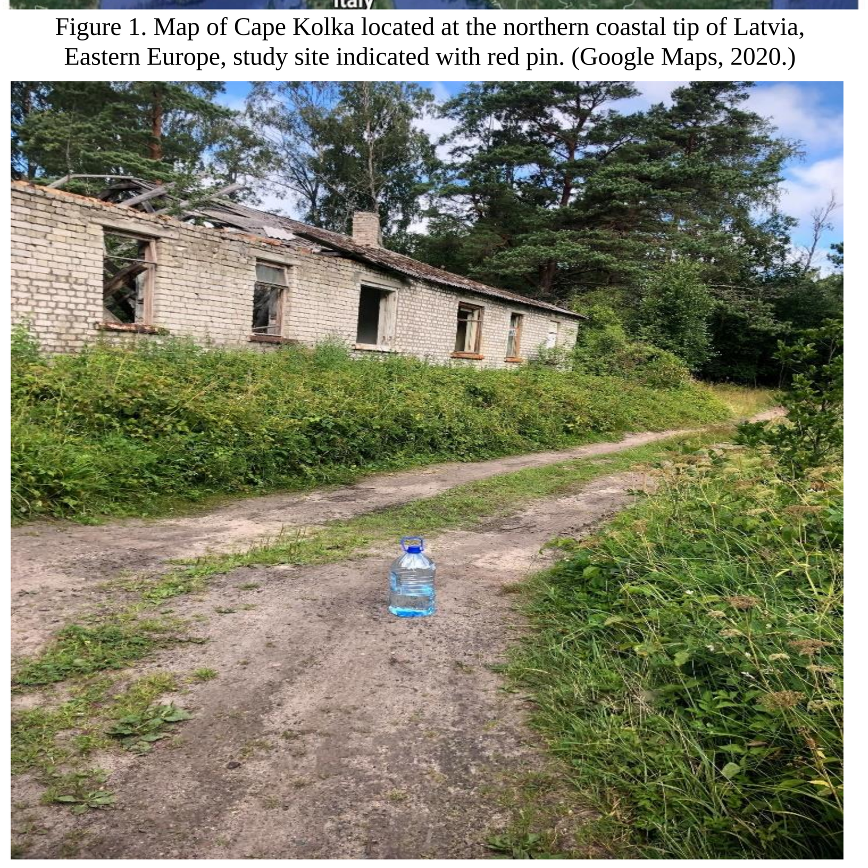

Figure 2. Deserted buildings where Soviet officers and their families occupied while at the beach.

In the last 50 years, the coastline has been experiencing an increase of cyclonic weather and strong wind currents causing redistribution of waves, leading to beach erosion and accumulation of sediments along different sections of the coast (Wolski and Wisniewski, 2020; Eberhards et al., 2009). Evidence of erosion and retreating coastlines caused by extreme weather and waves can be found along the southern Baltic coast, leaving exposed bedrock and sedimentary deposits. Going up north from the south, along the Baltic Sea coastline to Cape Kolka, is a prograding depositional strandplain that has formed due to strong winds on the Baltic Sea and longshore drift currents towards the northern tip that deplete large amounts of sand along the coastline (Eberhards et al., 2009).

Previous coastal subsurface investigations using GPR, Clemmensen and Nielsen (2010), Pitnam et al. (2019), and Vilumma et al. (2016) have progradational results in their research that I have used as a reference in my GPR profiles because the stratigraphic patterns are similar. Cape Kolka has a complex coastline provides a good opportunity to collect and interpret progradational coastal stratigraphic research using GPR.

Methodology

GPR is a noninvasive geophysical tool that has become popular in the last 25 years in geomorphic and stratigraphic research (Jol and Bristow, 2003). GPR provides shallow subsurface imagery by using different electromagnetic (EM) frequencies for investigating stratigraphy and sedimentary architecture in 2-D and 3-D perspectives (Jol and Bristow, 2003). The antennae at the surface uses an EM frequency wave that is transmitted through the subsurface and reflected back to the surface. The EM waves that are reflected back are received by an antenna and recorded. Different antennae frequencies help determine soil properties, continuity of reflections, and the resolution of the GPR profile (Jol and Bristow, 2003). Data that is received and recorded is then ready to be processed by software and interpreted using radar stratigraphic interpretation principles (Jol and Bristow, 2003).

The GPR data was collected along a 1,000 m line, on a sandy road that is relatively straight, meaning few sharp curves (figure 3). A Sensors and Software pulseEKKO Pro GPR system was used with 100 and 500 MHz frequencies and a topographic laser leveler. The sandy road goes through a wooded and marshy area that goes over ridges perpendicular to the general ridge direction of the strandplain. Table 1 shows the antennae separation and step size used for each frequency.

Table 1. Antennae separation and step size used for the 100 MHz and 500 MHz.

Frequency	Antennae separation	Step size
100 MHz	1.0m	0.25m
500 MHz	0.15m	0.01m

A common midpoint (CMP) survey was conducted for the 100 MHz system by increasing the space between the transmitter and the receiver with each step taken. CMP results are based on the calculation between the depth of penetration in the ground and the two-way travel time of the reflections to determine the radar signal velocity, in this study the velocity is 0.069 m/ns (Jol and Bristow, 2003). The GPR resolution distinguishes between the two-way travel time signals based on pulse widths and spatial pulse length. The resolution improves with higher frequencies if the width stays the same, therefore GPR can operate on different frequencies (Davis and Anna, 1989).

Collected data was processed through EKKO_Project 5 software that displays the stratigraphy reflections in the subsurface from the study area to analyze and interpret different sedimentary structures (Pitman et al., 2009). In order to create a geometrically correct high-resolution profile, topographic points were collected along the line using a TopCon RL-H3CL laser leveler at 5m intervals, placed into a table on Microsoft Excel, and combined with the GPR profile in EKKO_Project 5.

Results

The two GPR profiles (100 and 500 MHz) that were collected along the prograding Cape Kolka strandplain were used to analyze and interpret the reflections of the sand deposit layering in the subsurface (figure 3) (Kitenberga et al., 2019). The 100 and 500 MHz lines start at 0 meters, the beginning of the sandy road that is off the main road, P124, going north east to Cape Kolka and ends at 1,000 m going east towards the coastline (figure 3). Each profile given a closer look after being processed through EKKO_Project to capture main stratigraphic features present in coastal progradation.

Figure 3. Map of the GPR line where meters are indicated where the data was collected to analyze the stratigraphy of the GPR profiles in the subsurface.

The 500 MHz GPR profile has a velocity of 0.069 m/ns that was calculated using the hyperbola velocity calibration in EKKO_Project 5, a depth penetration of 1.5 m, and a clearer resolution that shows more detail compared to the 100 MHz profile. The profile shows a horizontal to sub horizontal reflection patterns which are mainly straight and parallel lines that indicate aggradation or increase in land surface.

The 500 MHz GPR profile has a velocity of 0.069 m/ns that was calculated using the hyperbola velocity calibration in EKKO_Project, a depth penetration of 1.5 m, and resolution the picks up more stratigraphy compared to the 100 MHz profile. The profile shows a horizontal to sub horizontal reflection patterns, mainly straight and parallel lines that are interpreted as aggradation or increase in land surface. Dipping reflections are visible throughout the profile and are interpreted as beachface deposits that have formed due to swash and backswash systems that occur due to wave activity (Clemmensen and Nielsen, 2010).

I have calculated the slope or angle of the dipping reflections using the expression in figure 4 provided by Sensors and Software, these angles range from 2 to 18 degrees. At 800 m til the end of the GPR line, we begin to see hyperbolas that are associated with roots from the vegetation growing close to the GPR line and infill at 530 m, 810 m, 858-886 m (figures 7 and 8).

$$\theta = \tan^{-1}\left(\frac{\Delta z}{\Delta x}\right)$$

Figure 4. Dip calculation expressed as change in depth (Δz) over horizontal distance (Δx) provided by the Sensors and Software website for tips on calculating dip angles (Sensors and Software, 2021).

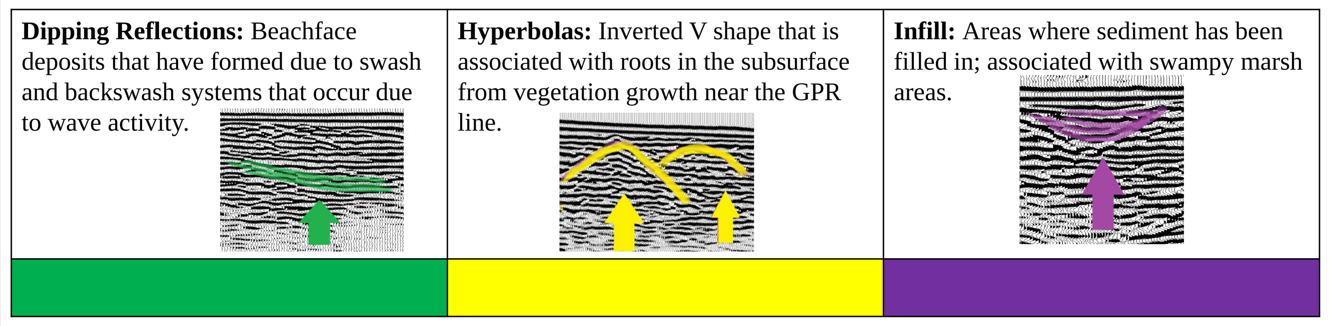

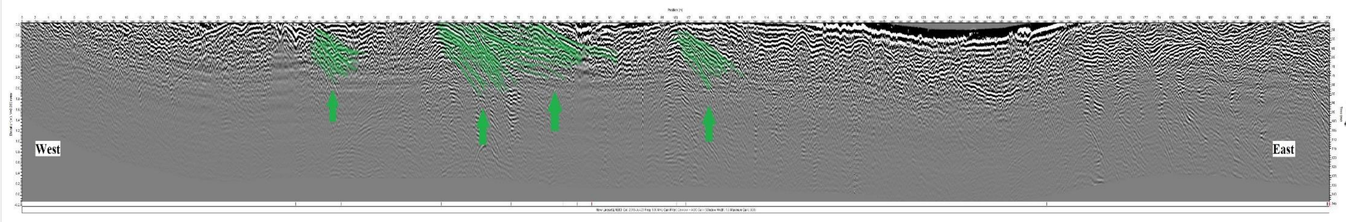

Figure 5. 0 to 200 m GPR profile, see figure 3 for GPR profile location. Going left to right, the first arrow has a reflection dip of 2°, the second 6°, the third 4°, and the fourth 4°. At 0 m the line starts at the end of the sandy road, off another main road. As meters increase, we are shooting the GPR west, towards the coast.

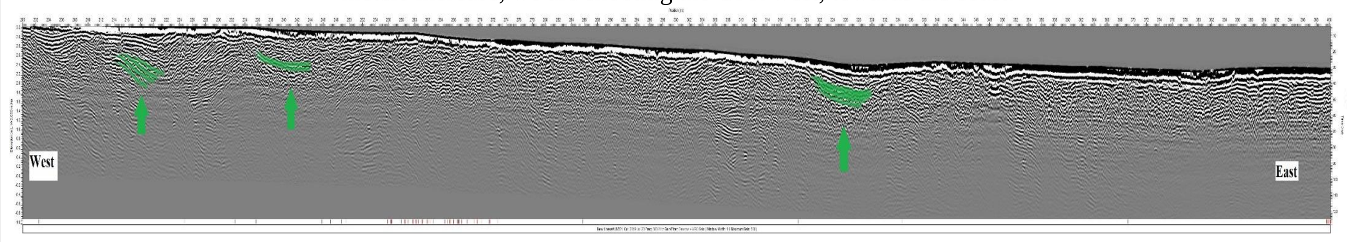

Figure 6. 200 to 400 m GPR profile with dipping reflections. The first green arrow has a dip of 4°, the second 3°, and the third 3°.

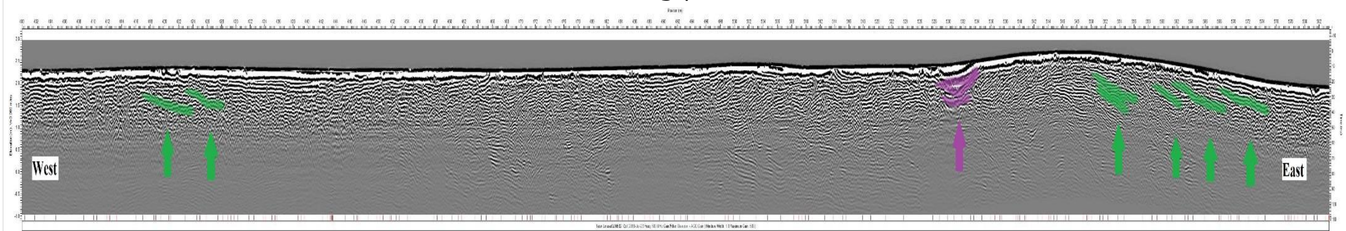

Figure 7. 400 to 600 m GPR profile with dipping reflections and infill between 528 m and 534 m. The first green arrow has a dip of 4°, the second 5°, the third 5°, the fourth 7°, the fifth 7°, the sixth 7°, and the seventh 2°.

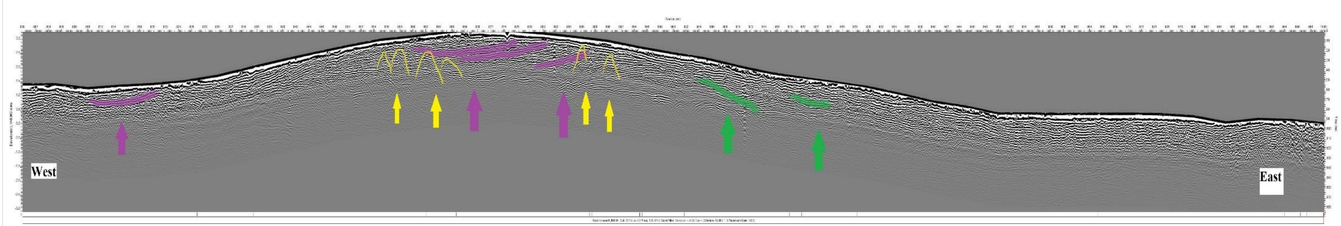

Figure 8. 800 to 1,000 m GPR profile with dipping reflections, infill, and hyperbolas. The first dip is 3° and the second is 3°. Infill may be due to potholes that have formed on the road and filled with sediment over the years. The hyperbolas are results from tree roots that have grown along the road.

The 1,000 m 100 MHz profile was separated into two different profiles, the first 100 MHz profile is 0 to 400 m (figure 9) and the second is 400 to 1,000 m (figure 10). This profile has a velocity of 0.069 m/ns that was calculated using the hyperbola velocity calibration in EKKO_Project, a depth penetration of 16 m where reflections are visible. About 70% of the 100 MHz profiles have horizontal to sub horizontal reflection patterns, mainly straight and parallel lines that are interpreted as aggradation or increase in land surface. Along with dipping reflections or slopes that have been interpreted as beachface deposits formed by swash and backswash systems due to wave activity (Clemmensen and Nielsen, 2010). Hyperbolas are found in the relative same location as the 500 MHz profile at 800 m and infill at 530 m, 810-820 m, 860-880 m, and 880-886 m (figure 10). Images and field notes have indicated trees close to the line suggesting that their roots are what we are seeing in the subsurface.

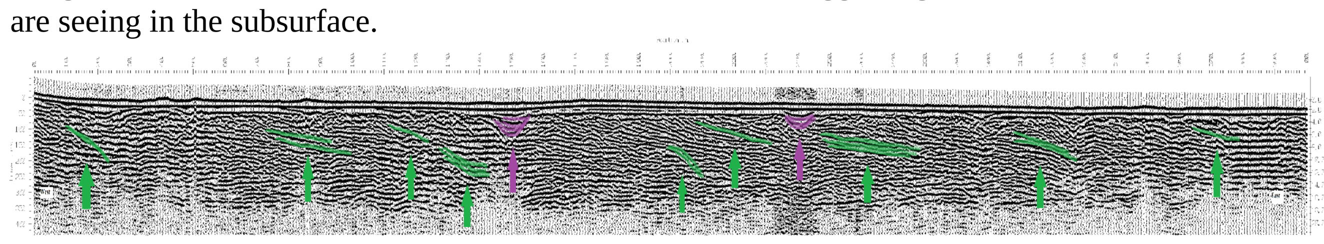

Figure 9. 0 to 400 m 100 MHz GPR profile shows dipping reflections and infill between 140 m and 160 m. The first green arrow has a dip of 18°, the second 4°, the third 8, the fourth 11°, the fifth 11°, the sixth 5°, the seventh 5°, the eighth 15°, and the ninth 8°.

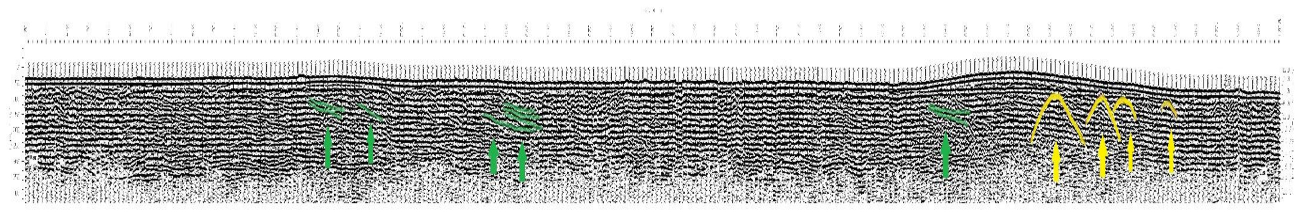

Figure 10. 400 m to 1,000 m 100 MHz GPR profile shows dipping reflections, with four hyperbolas between 890 and 950 m. The first green arrow has a reflection dip of 5°, the second 11°, the third 8°, the fourth 11°, and the fifth 5°.

Discussion

After analysis and interpretation of the 500 MHz and 100 MHz GPR profiles, there is evidence of coastal progradation from the dip ranges and aggradational patterns in the subsurface along the Baltic Sea near Cape Kolka. The dipping reflections in the 500 MHz and 100 MHz indicate that there is sediment being deposited, causing the sandy coast to prograde in width (Pitman et al., 2019). Infill found in figures 7, 8, and 9 are due to sediment filling in, this is associated with marshy areas. Hyperbolas are near 800 til the end of the survey line. Hyperbolas are theorized to be trees or roots in the subsurface that caused the electromagnetic waves to reflect off of it (Jol and Bristow, 2003). Figure 12 is a diagram showing an example of what roots look as hyperbolas in the subsurface (Guo et al., 2012).

Figure 11. An image at 160 m where infill is visible in the GPR profiles.

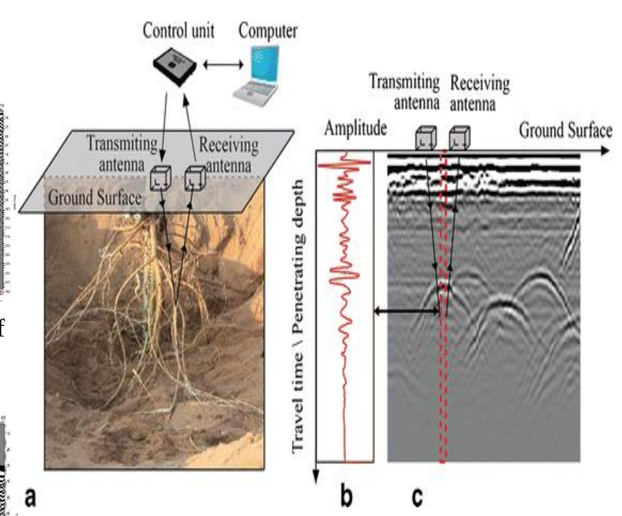

Figure 12. Diagram of roots in the subsurface using GPR (Guo et al., 2012).

Figure 13. The red arrows are used to indicate the trees that may have roots causing the hyperbolas in the subsurface.

Conclusion

The two GPR profiles that were collected at Cape Kolka were collected, collated, processed, and interpreted to get a better understanding of how the Baltic Sea coastline has been changing and prograding. After analyzing and interpreting the reflections within the GPR profiles, the profiles revealed dipping reflections, horizontal to sub horizontal patterns, hyperbolas, and infill. The dipping reflections have a range of dipping angles between 2 degrees and 18 degrees that dip towards the coast. Eroded sediment near Cape Kolka was deposited through longshore drift has built the coast out at the northern tip. The results provide imagery that suggests the coastline is prograding since the dipping stratigraphy go towards the coastline (east), and the study done by Clemmenson and Nielsen (2010) had similar results that indicate progradation. The Cape Kolka results may be useful for 1) researchers interested in GPR or prograding coastlines, 2) land developers who would like to develop on land similar to this site, 3) residents who live near Cape Kolka and how the coast is changing that may impact their livelihoods, 4) park management to help preserve and regulate activities near Cape Kolka and 5) tourists that visit Slitere National Park that would like to learn more about the environment.

Acknowledgements

We would like to acknowledge and give thanks to the University of Wisconsin- Eau Claire International Fellows Program (IFP) for funding and supporting international student-faculty collaborative research/creative activity and research service learning. Also acknowledge and give thanks to the University of Wisconsin- Eau Claire Student/Faculty Research Collaboration Program (Office of Research and Sponsored Programs) (ORSP) for funding opportunities. We would also like to acknowledge and give thanks to the Simpson Fund and the ORSP travel funding for making traveling, working, and collaborations possible. Finally, we would also like to acknowledge and give thanks to Dr. Donatas Pupienis, Professor in the Department of Hydrology and Climatology at the Vilnius University for traveling along and collaborating with us at Cape Kolka.

References

Buynevich, I., and Pupienis, D. 2007. Reactivation of coastal dunes documented by subsurface imaging of the Great Dune Ridge. *Journal of Coastal Research*, 50, 226–230.

Clemmensen, L. and Nielsen, L. 2010. Internal architecture of a raised beach ridge system (Anholt, Denmark) resolved by ground penetrating radar investigations. *Sedimentary Geology*, 223, 281-290.

Davis, J., and Annan, A.1989. Ground Penetrating Radar for High-Resolution Mapping of Soil and Rock Stratigraphy. *Geophysical Prospecting*, 37, 531-551.

Eberhards, G., Grine, I., Lapinskis, J., Purgalis, I., Saltupe, B., and Torklere, A. 2009. Changes in Latvia's seacoast (1935- 2007). *Baltica*, 22 (1), 11-22. Vilnius. ISSN 0067-3064.

Eberhards, G., Lapinskis, J., and Saltupe, B. 2006. Hurricane Erwin 2005 coastal erosion in Latvia. *Baltica*, 19 (1), 10–19. Vilnius. ISSN 0067-3064.

Fisher, S., Stewart, R., and Jol, H. 1992. Processing ground penetrating radar (GPR) data. *GPR Processing*, 4.

Google Maps, 2020, The Kolka Cape. (accessed September 2020).

Gu?, L., Chen, J., Cui, X., Fan, B., and Lin, H. 2013. Application of ground penetrating radar for coarse root detection and quantification: a review. *Plant Soil*, 362, 1-23. DOI: 10.1007/s11104-012-1455-5.

Kitenberga, M., Drobyshev, I., Elferts, D., Matisons, R., Adamovics, A., Katrevics, M., Niklasson, M., and Jansons, A. 2019. A mixture of human and climatic effects shapes the 250-year long fire history of a semi-natural pine dominated landscape of Northern Latvia. *Forest Ecology and Management*, 441, 192-201.

Jol, H., and Bristow, C. 2003. GPR in sediments: advice on data collection, basic processing, and interpretation, a good practice guide. *Ground Penetrating Radar in Sediments*, 211, 9-27.

Pitman, S., Jol, H., Shulmeister, J., and Hart, D. 2019. Storm response of a mixed sand gravel beach ridge plain under falling relative sea levels: A stratigraphic investigation using ground penetrating radar. *Earth Surface Processes and Landforms*, 44, 1610-1617. DOI: 10.1002/esp.4598.

Vilumaa, K., Tonisson, H., Sugita, S., Buynevich, I., Kont, A., Muru, M., Preusser, F., Bjursater, S., Vaasma, T., Vandel, E., Molodkov, A., and Jarvelill, J. 2016. Past extreme events recorded in the internal architecture of coastal formations in the Baltic Sea Region. *Journal of Coastal Research*, 75, 775-779. DOI: 10.2112/5175-156.1.

Wolski, T., and Wisniewski, B. 2020. Geographical diversity in the occurrence of extreme sea levels on the coasts of the Baltic Sea. *Journal of Sea Research*, 159.

Sensors and Software. 2021. Tips for Dips. (accessed September 2021).